Transactions, SMiRT-23
Manchester, United Kingdom - August 10-14, 2015
Division II, Paper 224

Ductile-brittle transition characterisation of NESC-I spinning cylinder steel using the small punch test

J. Adams[1], R. C. Hurst[1], J. B. Borradaile[2] and M. R. Bache[1]

[1] Institute of Structural Materials, College of Engineering, Swansea University, Singleton Park, Swansea, SA2 8PP, United Kingdom

[2] Rolls-Royce plc, P.O. Box 2000, Derby, DE21 7XX, United Kingdom

ABSTRACT

The small punch (SP) tensile test, originally developed for assessing the integrity of nuclear containments, has seen a renaissance in recent years with the introduction of a Code of Practice through CEN (2007) and a standardisation proposal. For nuclear applications, the extremely low volumes of material that are required allow specimens to be manufactured from quasi non-destructive scoop samples, surveillance specimens or even previously tested Charpy specimens. The low volume of material also alleviates the health and safety requirements and therefore the cost of testing radio-active materials. By assessing the energy absorbed before fracture, it is possible to build an entire SP ductile-brittle transition curve using less material than is required for a single Charpy test.
Small punch testing has been performed on the SA 508-3 NESC-I spinning cylinder material to establish ductile-brittle transition data. The extremely well characterised nature of the NESC material provides a good platform for comparisons to conventional Charpy impact test techniques. Multiple SP ductile-brittle transition curves have been constructed, building upon the framework of the existing Code of Practice. Novel geometries and associated machining techniques employed to incorporate notches into the surface of the SP specimen, together with the application of relatively high strain rates, are described. Post-test fractography illustrates the influence of both stress raising features and strain rate on small punch fracture behaviour, plus any effect on the SP/Charpy correlation 'α' factor. Finally the SP test enables comparisons against previously published NESC fracture data.

INTRODUCTION

The first research into small punch (SP) testing took place in the early 1980s, with two American laboratories, Manahan et al. (1981) and Baik et al. (1983) working together to determine stress-strain curves from very limited volumes of material. More recently, the technique is developing with increasing pace, as the advantages of small scale testing become more relevant across the conventional power generation, nuclear and aerospace sectors. Potential benefits to the modern nuclear industry continue to include the compatibility with scoop sampling and surveillance specimens, and reduced safety requirements and costs associated with machining and testing irradiated material.
The current research focused on material originally used by the Network for Evaluating Structural Components (NESC) as part of the international NESC-I spinning cylinder project (Bass, R. et al, 2001). The previous programme incorporated a wide range of non-destructive testing, as well as conventional mechanical testing, culminating in a large scale component validation test. The NESC A508 Class 3 reactor pressure vessel steel used for the present study is therefore extremely well characterised and has previously been subjected to small specimen testing by Turba et al. (2013).

The NESC-I project was organised to establish how best the integrity of a reactor pressure vessel (RPV) could be assured under both operating and postulated accident conditions. The culmination of this work led to the destructive testing of a large reactor pressure vessel (RPV) steel cylinder, complete with manufactured flaws and internal 316 stainless cladding. The A 508 Class 3 cylinder was

specially manufactured for tests designed to initiate cleavage crack growth as may occur in aged microstructures.

Previous studies which have attempted to utilise small punch samples to generate ductile to brittle transition data have failed to directly duplicate the Charpy derived transition temperature without the incorporation of a "correction factor, α". One argument put forward was that unlike the notch machined into a Charpy specimen, the small discs did not incorporate a stress raising feature where a degree of local plastic constraint was concentrated (Turba et al. 2011). Albeit for a different alloy, the same authors attempted to circumvent this by employing small punch specimens containing a concentric groove. A direct relationship to Charpy ductile-brittle data remained elusive, however. The concept of a notched or cracked small punch specimen is not new in itself, but the method is often intricate or elaborate; sharp, circular EDM notches, from Turba et al. (2011), through specimen slots from Lacalle et al. (2008) and Cuesta et al. (2011) and laser-induced micromachining (Ju et al. 2003) have all been investigated in recent years. Another explanation often used to explain the 'alpha' factor is the vast difference in strain rates between SP and Charpy testing. The Code of Practice (CEN (2007)) suggests a punch displacement rate between 0.2mm/min and 2mm/min be employed.

The objective of the current study was to investigate whether the introduction of linear forms of stress raising features onto the surface of the disc specimen, and increased strain rates, could result in ductile to brittle transition behaviour more in line with the original NESC-I fracture data. Two methods of introducing a notch onto the surface of a specimen were examined. Firstly a scratching process was considered potentially easier to introduce to irradiated material and requiring less preparation, while avoiding the thermal damage inevitable with other preparatory processes such as electro-discharge machining. Secondly an EDM notch as used by Matocha et al (2014) and Kim et al. (2005) was also tested allowing material specific comparisons to be drawn.

MATERIAL, SPECIMEN PREPARATION AND EXPERIMENTAL PROCEDURE

A section of the original NESC-1 material was supplied by the Joint Research Centre (JRC), Petten, who previously managed the NESC Network. The chemical composition is given in Table I. Testing carried out as part of the NESC-I programme showed that the heat affected zone (HAZ) resulting from the internal vessel cladding was between 7.5mm and 8.8mm in depth. The material extracted for this research was therefore taken from a region between 30mm and 40mm from the cladding. Cylindrical blanks of 9.5mm diameter were removed from the parent material by EDM with their longitudinal axis parallel to the longitudinal axis of the pressure vessel wall. This orientation allowed the disc specimens to be prepared so that fracture could occur on the same plane as the original specimens tested as part of the NESC project, providing a stronger position from which comparisons against conventional specimens could be drawn. The cylindrical blanks were sectioned into thin discs using a precision cutting wheel, before grinding to final thickness. In accordance with the CEN Workshop Agreement (CEN (2007)), the discs were ground to a thickness of 0.5mm with a minimum final grinding stage using 1200 grit SiC paper. Measurements were taken at four opposing points across the specimens to verify a tolerance of ±0.5%. At this stage, two orthogonal scratches were introduced to one surface of one quarter of the specimens, transecting in the centre of the disc to form a cross (Figure 1). These scratch-type notches were formed with multiple passes of a tungsten-carbide tool with a tip radius of approximately 40μm, to a nominal depth of 50μm. Figure 2 illustrates a metallographic cross-section taken orthogonal to a typical scratch. A single notch passing through the centre of the specimen was introduced to another quarter of the specimens using EDM (Figure 3). Figure 4 shows the profile of this 'U' shaped notch with a depth of 200μm and a tip radius of 125 μm.

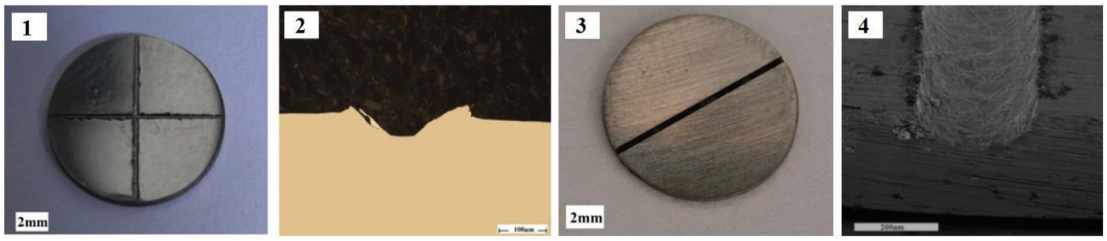

Figures 1-4. Notched small punch specimens

Testing was performed using a servo-hydraulic testing machine, fitted with a 25kN load cell. The machine was integrated to an environmental chamber, with a working temperature range of -170°C to +300°C. Modifications to the load train were made, allowing the jig to be fully submersed in liquid nitrogen while in the chamber to achieve even lower test temperatures. A calibrated T-type thermocouple, positioned in a recess on the surface of the jig was used for temperature measurement. A Nimonic 90 punch with a 2.5mm diameter hemispherical tip was used for the Small Punch test, with the specimen gripped between the die leaving a 4mm aperture.

Table 1. Composition of NESC-I SA 508 Class 3 material

	C	Si	Mn	S	P	Cr	Mo	Ni	Fe
Wt %	0.23	0.23	1.32	0.011	0.012	0.08	0.50	0.73	Bal

Testing was conducted at seven specific temperatures, selected to encompass both upper and lower shelf behaviour. The same temperatures were used for both plane and scratched specimens and high strain rate testing to allow direct comparisons to be made. At most temperatures, duplicate tests were performed where possible, to establish the repeatability of the technique. Following testing, specimen fracture surfaces were examined using a scanning electron microscope (SEM). Attention was focussed on both the macroscopic deformation of the disc and the microscopic fracture surface appearance.

RESULTS

Plane Disc Tests

Initial testing on plane specimens was undertaken at a punch displacement of 0.3mm/min and produced an obvious transition from ductile to brittle behaviour across a temperature range of 21°C to -196°C (294K to 77K). Figure 5 shows typical load displacement traces used to derive the transition curve. The tests with fracture energies lying on the upper shelf exhibited a distinct peak load after which the load dropped gradually before ultimate failure. The peak load measured from individual tests can be seen to increase, as expected, as the material strengthens with decreasing temperature. Towards the transition temperature, failure was more sudden as the effects of the strengthening becomes less prominent than the loss of ductility. At even lower temperatures, it was noted that the initial fracture event occurred at relatively low loads with multiple load drops detected after the initial cracking.

One of the key elements in analysing the data from these tests was selecting a point to determine where failure is believed to have occurred. As such, changing this point gives varying bias to different fracture modes across the temperature range. The various methods include taking the maximum load, the point of first load drop or after a cumulative 20% load drop. The Code of Practice (CoP) states that the area under the curve should be taken up to a point 20% beyond the peak load (i.e. $F_f = 0.8\ F_m$), but this approach is not always taken. Following the CoP (Anon 2007), as opposed to taking the highest load, gives higher fracture energies for tests failing with ductility or multiple drops, whilst having minimal effect on more sudden failures towards the transition region. Figure 6 shows the ductile to brittle transition temperature (DBTT) curve produced from this series of tests. In calculating the fracture energies, the area under the load-displacement curve for each specimen was calculated up to the maximum load, or to the first indication of fracture for specimens indicating multiple fracture events. The small punch transition temperature (T_{SP}) estimated from this data is -128°C, taking a mean upper and lower shelf value. This corresponds well with the literature ((Hurst & Matocha (2014), Brezina et al. (2014), Matocha et al. (2014), and particularly Turba et al (2013) who quoted a T_{SP} of -137°C for the same material.

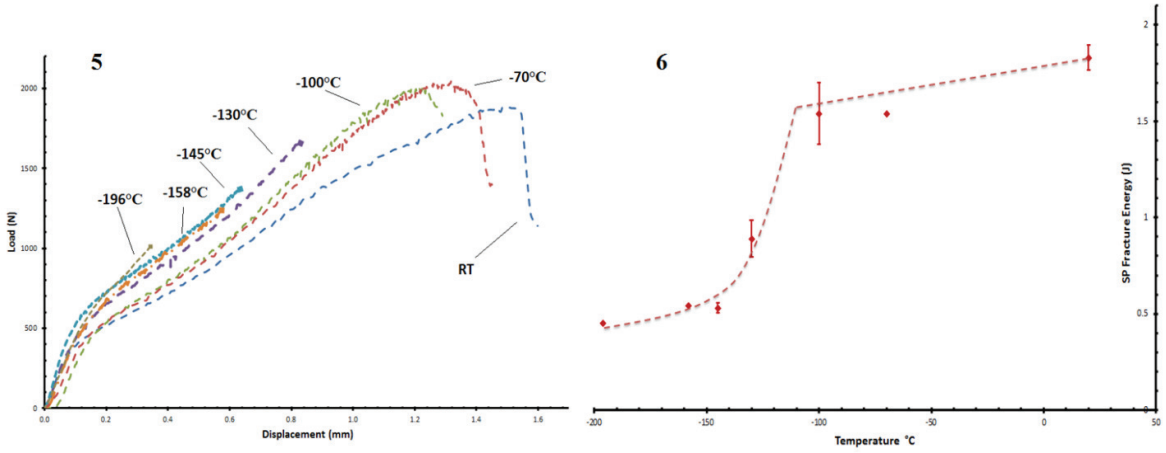

Figures 5 and 6. Typical load displacement and ductile to brittle transition curves for plane specimens (RT to -196°C).

High Strain Rate

Figure 7 shows the DBTT curve for plane specimens tested at high strain rates with a punch displacement rate (PDR) of 100mm/s. Comparing this to Figure 6 reveals some clear differences. The upper shelf has a negative gradient, with a pronounced drop into the transition region. The energy absorbed during fracture is also generally higher than at lower strain rates for all temperatures, with the exception of tests carried out at -196°C. The transition temperature ($T_{SP,HSR}$) for this series of tests was -159°C; a shift towards lower temperature of 31°C from the testing carried out at rates in line with the CoP..

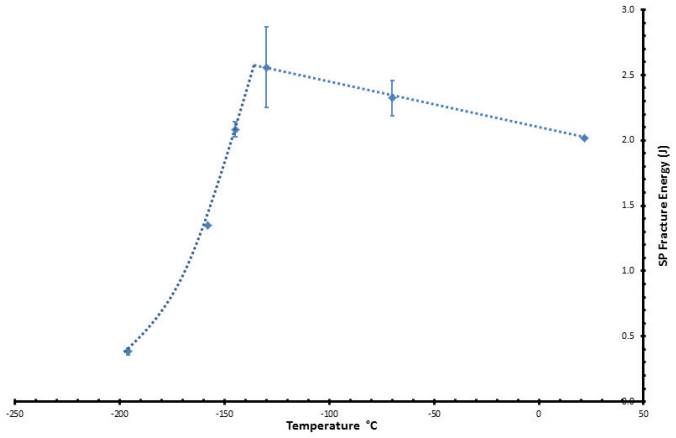

Figure 7. Ductile-brittle transition curve for testing of plane specimens at a PDR of 100mm/s

Examination of the microscopic fracture surface is a useful means of evaluating fracture behaviour from SP testing. Figures 8 and 9 show the fracture surfaces of specimens tested in line with the COP and at increased PDRs. At -130°C, conventional testing has yielded a mixed mode fracture. Brittle faceting can be seen, along with localised evidence of micro-void coalescence. This is consistent with testing that produced a T_{SP} of -128°C. At increased strain rates, however, the fracture surface is dominated entirely by ductile micro-voids. Similarly, at -158°C the high strain rate specimen does not show a fully brittle facetted surface like the specimen subjected to conventional punch displacement rates.

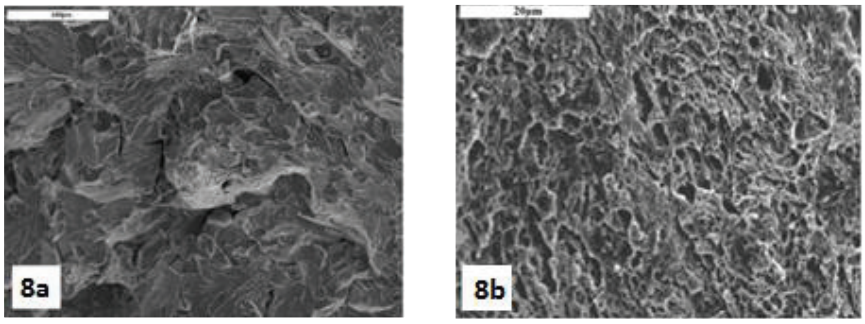

Fig 8. Low (a) and high strain rate (b) fracture surfaces tested at -130°C

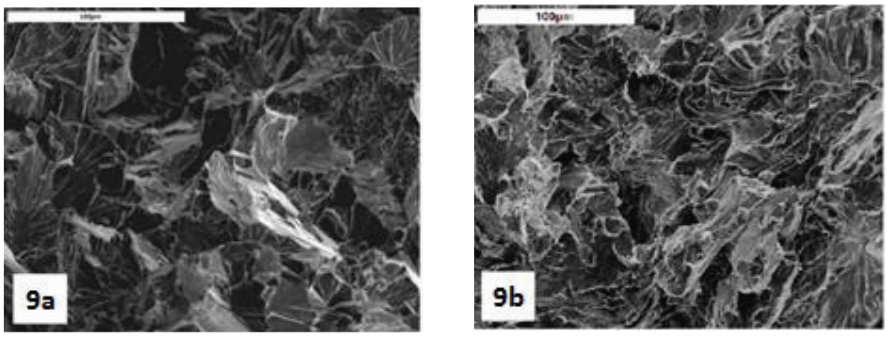

Fig 9. Low (a) and high strain rate (b) fracture surfaces tested at -158°C

Notched Specimens

Following the testing of plane specimens in line with the COP and at increased strain rates, the novel notch geometries were studied. Figure 10 shows the DBTT curve constructed using the EDM notch shown in Figures 3 and 4. The trend is very similar to previous curves, but with a narrower and more sudden transition and a drop in the lower shelf energies. The amount of energy absorbed during fracture is less across all temperatures, with only 0.06J absorbed at -196°C, compared to 0.45J in the plane specimens. The upper shelf shows a negative gradient, while a transition temperature ($T_{SP(notched)}$) of -133°C was established.

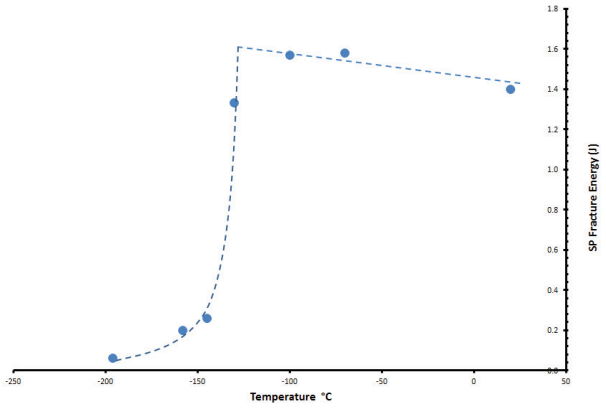

Fig 10. Ductile-brittle transition curve for testing of EDM 'U' notched specimens

Figure 11 shows the DBTT curve constructed following testing of the scratched specimens alongside the data from the EDM notched samples. It can be seen that the introduction of the different stress raising features has had a similar effect, with consistent transition and lower shelf behaviour. The upper shelves are parallel, but with the scratched samples absorbing more energy. A $T_{SP(scratched)}$ of approximately -131°C was established with the scratched samples.

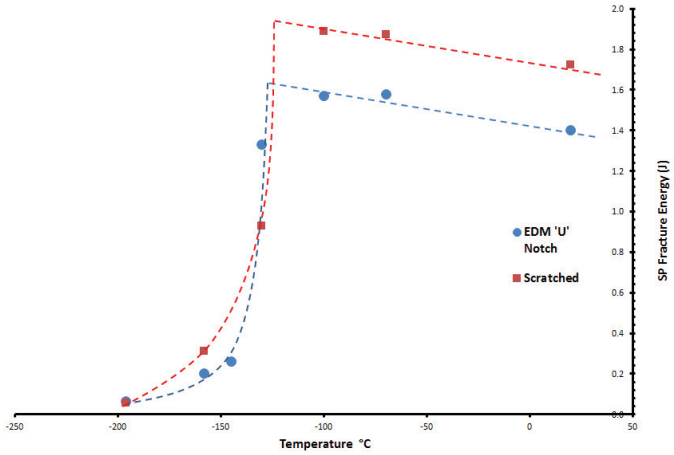

Fig 11. Comparison of DBTT curves for notched and scratched specimens

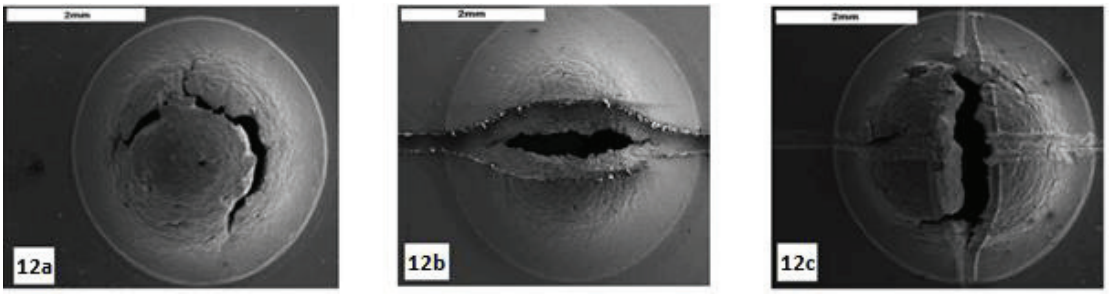

Fig 12. Typical plain (a), notched (b) and scratched (c) specimens tested at RT

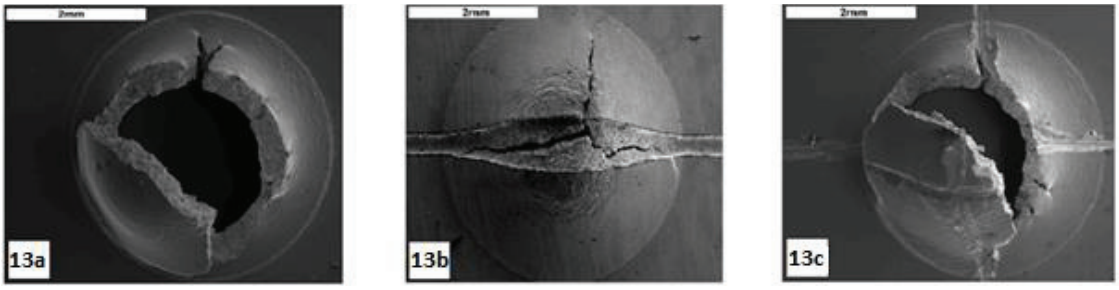

Fig 13. Typical plain (a), notched (b) and scratched (c) specimens tested at -130°C

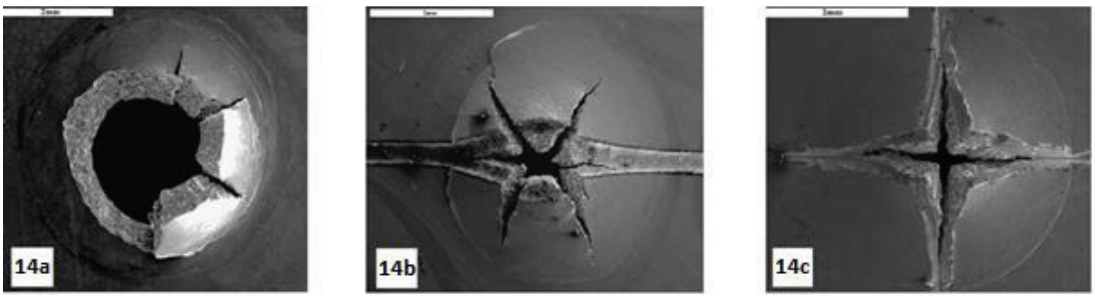

Fig 14. Typical plain (a), notched (b) and scratched (c) specimens tested at -196°C

Figures 12 to 14 show macroscopic fracture mechanisms for the two different notch geometries presented, alongside the plane specimens previously described. These images illustrate the influence of the notches on fracture as mechanical properties change with temperature. The two ductile fractures from notched specimens tested at room temperature shown in Figure 12 appear quite similar. The effect of the scratch in influencing the crack path was more dominant for the deeper EDM notch. For the scratched specimen, the circumferential necking mechanism seen in Figure 12a appears to have been drawn up to the root of the notch. The typical circumferential cracking seen in the plane specimens prevails in the scratched specimen at -130°C (Fig. 13c). Figure 13b suggests the single 'U' shaped EDM notch has a more significant influence under these conditions. One crack can be seen to have propagated along the root of the notch, with another large crack runs perpendicular to it.

At -196°C, the notches are seen to have the greatest influence on fracture behaviour. Neither of the notched specimens tested at this temperature show any circumferential cracking, and there is much less plastic deformation evident on the surface within the 4mm recess. The four radial cracks seen in Figure 14c suggest a greater sensitivity to the novel scratches with the material in such a brittle lower shelf condition. This specimen shows no circumferential cracking; four radial orthogonal cracks follow the root of the notch and are of approximately equal length. Figure 14b shows a crack of similar length to that in Figure 13b running along the root of the 'U' notch. The fracture is dominated, however, by four radial cracks running away from the notch to form a 'star' type failure.

DISCUSSION

The fracture energies together with Figures 8 and 9 suggest that both upper and lower shelf behaviour was achieved within the temperature range used for these experiments. From a technical viewpoint, an extremely low temperature of -196°C was achieved by the use of liquid nitrogen for the current test matrix, however, even this capability could be insufficient should testing of a material with an even lower T_{SP} than found in the present work be required. It is well understood that transition temperatures generated from SP testing can be significantly lower than those obtained from conventional Charpy testing. This is true for both DBTT and fracture appearance transition temperature (FATT) data. An empirical correlation factor has been developed (CEN (2007)) which attempts to relate these two values such that:

$$\alpha = \frac{T_{SP}}{T_{CVN}} \ (K) \qquad (1)$$

Comparison with Conventional NESC Data

As part of the NESC-I spinning cylinder project, Charpy impact testing was carried out in line with DIN 50115 and ESIS Draft 9 across a temperature range of 20°C to 150°C (Rintamaa & Planman 2000). This resulted in a transition temperature at 41 joules of T_{41J} = 78°C and a 50% fracture appearance transition temperature (FATT) or T_{FATT} = 92°C. The difference between this data and the transition temperatures established using the small punch technique can be described by Equation 1. Hence, alpha factors for the NESC material can be calculated: α_{plane} = 0.42 and $\alpha_{plane,\ HSR}$ = 0.32. The conventional strain rate testing is consistent with both Turba et al (2013) and Kim et al (2005) who have performed similar tests, resulting in correlation factors ranging from α = 0.36 to α = 0.43. Alpha factors for notched samples were also established: $\alpha_{scratched}$ = 0.40, $\alpha_{notched}$ = 0.40.

The difference in strain rate between relatively slow small punch testing and high strain rate impact testing is often used to explain the necessity of the alpha factor (Turba et al. (2011) and Baik et al. (1986)). It was anticipated that increasing the punch displacement rate from 0.3mm/min to 100mm/s would yield an increase in the small punch transition temperature as a result of increasing yield stress. High strain rate testing has however shown a decrease in the alpha factor. This shifting of the transition temperature away from Charpy was not predicted. Following fractographic examination (Figures 8 and 9), it is proposed that an adiabatic heating effect may have been induced. A T_{SP} shift of

approximately 30°C is consistent with forging simulations at comparable actuation rates (Li et al. (2009)). This is also supported by the similarities between the fracture surfaces of 0.3mm/min testing at -130°C and 100mm/s testing at -158°C (Figures 8a and 9b), a difference of 28°C.

In manufacturing the novel scratched and notched specimens, it had been anticipated that the transition temperature could be shifted towards conventional testing by means of the notch, resulting in a higher correlation factor. The EDM notch geometry has been tested previously in the literature. Hurst & Matocha (2014) studied manufactured identical specimens from 14MoV6-3 pipe steel. The results for this material showed a much greater sensitivity to the notch. Firstly, the fracture energies for the notched specimens were consistently less than half that of a plane specimen across the entire temperature range. Secondly, it was noted that the introduction of the notch significantly shifts transition temperatures to higher values, and that the temperature dependence of fracture energy is less steep.

Small punch testing also allows tensile properties to be determined. For example, Mao and Kameda (1991) developed a formula allowing yield strength to be derived from a standard SP test for a variety of steel alloys (Equation 2).

$$\sigma_Y = \frac{360 L_Y}{t^2} \qquad (2)$$

Where L_y = SP elastic-plastic transition load and t = SP sample thickness. Taking this data from the room temperature load-displacement trace shown in Figure 5, Equation 2 gives a correlated yield stress of 558 MPa. Conventional tensile testing in line with BS EN 10 002, undertaken as part of the NESC-I project, produced an average yield stress of 567 MPa at room temperature.

CONCLUSIONS

Small punch specimens manufactured from NESC-I SA 508-3 reactor pressure vessel steel were tested under novel conditions and compared with original NESC fracture data: plane specimens were tested at very high strain rates, and two notch geometries were introduced onto the surface of a number of specimens. All samples were tested across a range of temperatures to examine ductile to brittle transition behaviour. Following testing, samples were subjected to fractographic examination to help correlate fracture energies with different fracture mechanisms. The following conclusions can be made:

- Small Punch specimens were tested at punch displacement rates of 0.3mm/min and 100mm/s. This resulted in transition temperatures of: $T_{SP,0.3mm/min}$ = -128°C, $T_{SP,100mm/s}$ = -159°C respectively.
- This decrease in the small punch transition temperature at high strain rate of 31°C has been attributed to an adiabatic heating affect.
- Two novel notch geometries were also introduced onto the surface of small punch specimens. These resulted in transition temperatures: $T_{SP(notched)}$ = -133°C and $T_{SP(scratched)}$ = -122°C.
- The most significant difference between plane and scratched/notched specimens was observed at -196°C, where neither scratched nor notched specimens failed with a typical large circumferential crack.
- Neither the increased strain rate nor the introduction of notches was found to raise the ductile brittle transition temperature towards the levels observed in conventional Charpy testing as part of the NESC-I project.

- Finally, a very good correlation with yield stress data from the original NESC-I project was found using the formula presented by Mao and Kameda (1991).

ACKNOWLEGMENTS

The current research was funded under the EPSRC Rolls-Royce Strategic Partnership in Structural Metallic Systems for Gas Turbines (grants EP/H500383/1 and EP/H022309/1). The provision of materials and supporting information from Rolls-Royce plc and the manufacturing support from MMR Ltd is gratefully acknowledged. Mechanical testing was performed at Swansea Materials Research and Testing Ltd. (SMaRT).

REFERENCES

Baik, J.M., Kameda, J. & Buck, O., (1986). Development of small punch tests for ductile-brittle transition temperature measurement of temper embrittled Ni-Cr steels. ASTM STP 888, pp.92–111.

Baik, J.M., Kameda, J. & Buck, O., (1983). Small Punch Test Evaluation of Intergranular Embrittlement of an Alloy Steel. Scripta. Met., 17, pp.1443–1447.

Bass, R. Wintle, J. Hurst, R. C. Taylor, N., (2001). NESC-1 Project Overview, Petten: European Coimmission.

Brezina, M. et al., (2014). Determination of Mechanical Properties of VVER-440 Reactor Pressure Vessel Steels after Irradiation in the Halden Reactor. In Determination of mechanical properties of materials by small punch and other miniture testing techniques. 2nd International Conference SSTT. pp. 112–118.

CEN, (2007). CEN Workshop Agreement - Small Punch Test Method for Metallic Materials CWA 15627,

Cuesta, I.I. et al., (2011). Analysis of different techniques for obtaining pre-cracked/notched small punch test specimens. Engineering Failure Analysis, 18(8), pp.2282–2287.

Hurst, R.C. & Matocha, K., (2014). Experiences with the European Code of Practice for Small Punch Testing for Creep, Tensile and Fracture Behaviour. In Determination of mechanical properties of materials by small punch and other miniature testing techniques. International Conference SSTT2014. pp. 1–26.

Ju, J.-B., Jang, J. & Kwon, D., (2003). Evaluation of fracture toughness by small-punch testing techniques using sharp notched specimens. International Journal of Pressure Vessels and Piping, 80(4), pp.221–228.

Kim, M.-C., Oh, Y.J. & Lee, B.S., (2005). Evaluation of ductile–brittle transition temperature before and after neutron irradiation for RPV steels using small punch tests. Nuclear Engineering and Design, 235(17-19), pp.1799–1805.

Lacalle, R., Álvarez, J. a. & Gutiérrez-Solana, F., (2008). Analysis of key factors for the interpretation of small punch test results*. Fatigue & Fracture of Engineering Materials & Structures, 31(10), pp.841–849.

Li, Y.P., Matsumoto, H. & Chiba, a., (2009). Correcting the Stress-Strain Curve in the Stroke-Rate Controlling Forging Process. Metallurgical and Materials Transactions A, 40(5), pp.1203–1209.

Manahan, M.P., Argon, A.S. & Harling, O.K., (1981). The development of a miniaturized disk bend test for the determination of post-irradiation mechanical properties. Journal of Nuclear Materials, 104, pp.1545–1550.

Matocha, K. et al., (2014). Comparison of Empirical Correlations for Determination of Tensile and Fracture Characteristics of Low Alloys CrMoV Steel in the Frame of Czech

Chinese Scientific Cooperation. In Determination of mechanical properties of materials by small punch and other miniature testing techniques. 2nd International Conference SSTT. pp. 142–149.

Mao, X. & Kameda, J., (1991). Small-punch technique for measurement of material degradation of irradiated ferritic alloys. *Journal of Materials Science*, 26(9), pp.2436–2440.

Rintamaa, R. & Planman, T., (2000). TG2 - Final report on Material Characterisation, NESC DOC TG 2,

Turba, K. et al., (2011). Introduction of a new notched specimen geometry to determine fracture properties by small punch testing. Engineering Fracture Mechanics, 78, pp.2826–2833.

Turba, K., Hurst, R. & Hähner, P., (2013). Evaluation of the ductile-brittle transition temperature in the NESC-I material using small punch testing. International Journal of Pressure Vessels and Piping, 111-112, pp.155–161.